Available online at www.sciencedirect.com
ScienceDirect
Nuclear Physics B Proceedings Supplement 00 (2012) 1–13
Nuclear Physics B Proceedings Supplement

Monte Carlo Event Generators

Stefan Gieseke

Institut für Theoretische Physik, Karlsruhe Institute of Technology, 76128 Karlsruhe, Germany

Abstract

We describe progress in the development of Monte Carlo event generators for the full simulation of collider physics events on the hadron level. We briefly comment on all areas of simulation but focus on the matching of higher order perturbative matrix elements and developments in multiple partonic interaction models.

Keywords: Monte Carlo, Event Generators, Next-to-leading order, Underlying Event

1. Introduction

Monte Carlo (MC) event generators have become an indispensible tool for analysing data from recent collider experiments. In the past decade the main multipurpose event generators HERWIG and PYTHIA [1, 2, 3] have been completely rewritten [4, 5] and a new generator, SHERPA [6, 7] has been established.

In this contribution we would like to summarize the most important developments that have been made in order to meet the requirement of increased theoretical precision. Furthermore, early data from the Large Hadron Collider (LHC) has triggered new developments in the modelling of the Underlying Event. Many details will be limited to the development of the HERWIG++ event generator.

In Fig. 1 we sketch the important simulation steps during the course of event generation. We start out with the hard scattering event (central blob), which describes the part of the simulation that happens at very short distances and is assumed to factorize from the rest of the event description. The distribution of energies and relative angles of typically a handful of particles is obtained from a Feynman diagram description of the physical subprocess. However, the particles in the final state are observed hadrons and will only be described by long–distance physics. To bridge this gap, parton showers evolve the final state from the hard (short disctance) scale Q to a small scale $Q_0 \sim 1\,\mathrm{GeV}$, thereby emitting mostly collinear and soft gluons from all coloured particles of the hard subprocess in the initial and final state. At this scale, the perturbative domain ends and the partonic degrees of freedom are converted into hadrons (circles in the final state) via a hadronization model, the cluster hadronization model in this case (white blobs). Finally, many of the created hardons are unstable, short-lived resonances that decay, possibly via other unstable hadrons, into stable particles, that live long enough to be probed by the detectors. In addition to this sequence of physical processes, all triggered by the hard subprocess, there may be additional (not so) hard processes, also called multiple partonic interactions. These are mostly fairly soft QCD interactions that also undergo parton showering etc. and produce additional particles in all the available phase space, although most of this activity will be found in the forward region.

Email address: stefan.gieseke@kit.edu (Stefan Gieseke)

2. Hard process and parton showers

The simulation of tree level processes with the available event generator programs is straightforward. SHERPA already comes with the automatic matrix element generators COMIX [8] and AMEGIC++ [9]. These are capable of generating matrix elements of in prin-

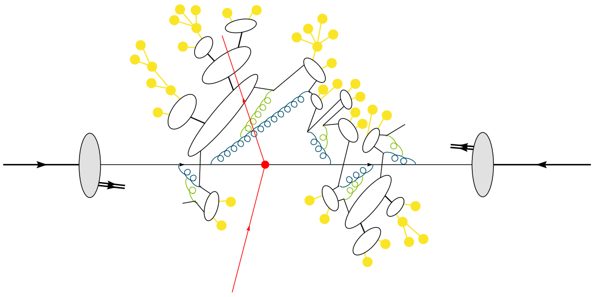

Figure 1: Sketch of the simulation of a typical hadron collider event.

ciple arbitrary complexity. The performance of generating events efficiently is, however, limited by the phase space generation to processes with typically 8-10 particles in the final state. PYTHIA and HERWIG come with a number of processes built-in. These contain most of the interesting standard model processes. Physics beyond the standard model can also be modeled in both programs [10, 11, 12]. In HERWIG, complex processes are being built-up automatically from simple $2 \to 2$ processes, followed by hard $1 \to 2$ and $1 \to 3$ body decays, based on the narrow width approximation for heavy intermediate particles. Spin correlations are restored to a good approximation, based on the algorithm described in [13]. In addition, events that cannot be handled directly by the latter two generators, can be generated with standard matrix element generators like MADEVENT [14] and written to event files in the Les Houches Event File (LHEF) format specified in [15]. These files contain unweighted events that are specified in sufficient detail such that they can be read in by the standard event generators which apply parton showers and hadronize the partonic final states.

The parton shower evolution has been newly formulated in various ways throughout all the event generators during the last decade. The development of HERWIG++ was based on the reformulation of angular ordered parton showers for massive particles [16]. PYTHIA now uses transverse momentum ordered parton showers that are interleaved with multiple partonic interactions [17, 18]. SHERPA by default has a parton shower evolution [19] based on Catani–Seymour Dipole subtraction terms [20]. Alternatively SHERPA has implemented a shower [21] that is based on dipoles similar to the ones used in the ARIADNE program [22]. Showers based on subtraction terms have been worked out by other groups [23] and also HERWIG has one implemented [24]. The VINCIA approach [25, 26, 27] employs antenna subtraction terms to formulate the parton showers and is available as an add-on module for PYTHIA. The motivation behind the reformulation of parton showers, based on subtraction terms for NLO calculations is the anticipated simplicity of matching fixed order calculations to the parton shower algorithm. This will be discussed in more detail below.

Fig. 2 compares the central transverse thrust, measured by CMS [28] to different event generator programs. As already known from LEP, the event generators are very well capable to describe this overall event structure. Parton shower and hadronization parameters are usually tuned to event shape data from LEP. The same quality of description is achieved at hadron colliders. The same holds for the integrated jet shapes, cf. Figs. 3 and 4. Here, the internal energy flow within a single jet of given radius R is measured. $\Psi(r)$ is the total energy of all particles in the jet with readius smaller than r. It is expected that this observable, mostly given by collinearly emitted particles is well described by parton showers and the subsequent hadronization models. This is indeed the case. One should note, however, that at hadron colliders the underlying event contributes significantly to the energy flow in each jet. Without a reasonable modeling of this, the description would never be as accurate as shown in the Figure.

3. Hard radiation

When considering harder radiation than in the previous section, the parton shower models still do sometimes remarkably well but often need to be supplemented with additional information about the momentum distribution of the hard particles. This is to a first approximation given by the matrix elements which in turn are calculated from Feynman diagrams. The parton showers only include information about the soft and collinear part of these matrix elements and hence are not sufficient to describe this alone. The first step towards including hard radiation are so-called hard matrix element corrections [31, 32]. The description of the high p_T tail of the transverse momentum spectrum of vector bosons in hadronic collisions can not be described by parton showers because the phase space that is accessible for hard gluon radiation is not sufficient. This can be corrected by filling in the phase space for hard radiation 'by hand' with the hard matrix element. Once corrected for the first hard emission, the approach breaks down already for the second hardest emission and so forth.

The inclusion of matrix element information for multiple hard radiation has been achieved in the CKKW approach [33, 34, 35]. The algorithm merges tree level matrix elements for a given process B and all subse-

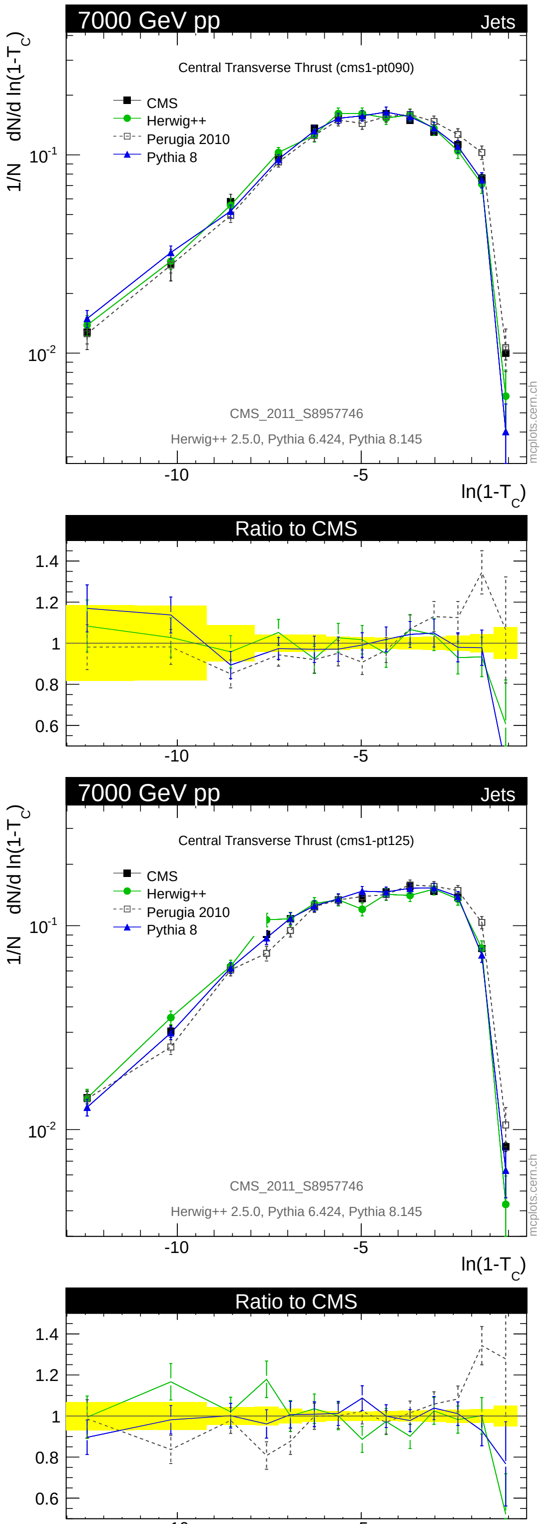

Figure 2: Transverse Thrust distribution from CMS [28] compared to different event generators [29], (top: $90 < p_T/\mathrm{GeV} < 125$, bottom: $125 < p_T/\mathrm{GeV} < 200$).

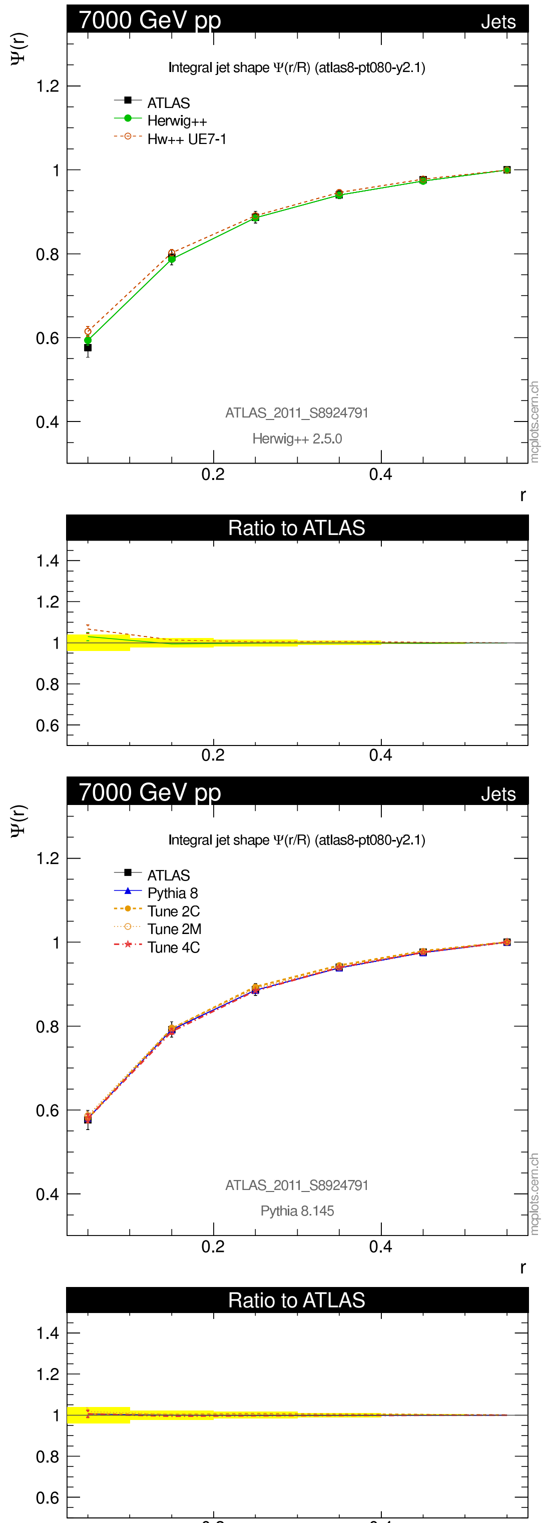

Figure 3: Integrated jet shapes from ATLAS [30] compared to different generators ($80 < p_T/\mathrm{GeV} < 110$; $1.2 < |y| < 2.1$) [29].

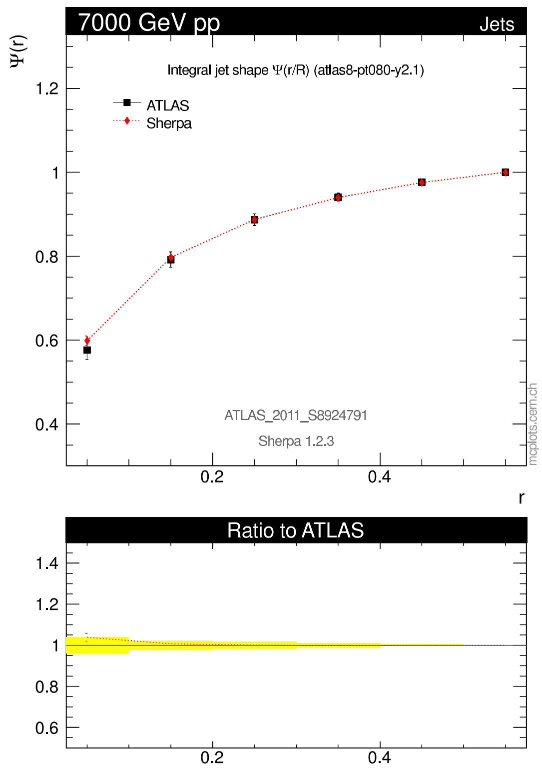

Figure 4: See caption of Fig. 3.

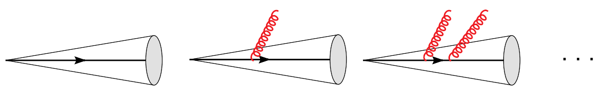

Figure 5: Sketch of leading process and processes with additional hard radiation. The cone denotes the different domains of parton shower and hard radiation, characterized by the separation scale $Q_{\rm ini}$.

quent processess with a maximum of n additional hard partons, cf. Fig. 5.

The hard radiation is separated from soft and collinear radiation by a merging scale $Q_{\rm ini}$ below which we trust the description of the parton shower and above which the additional information from the hard matrix elements should be used. Now, the rates for matrix elements with m additional hard jets that are resolvable above $Q_{\rm ini}$ are calculated on the basis of the leading logarithmic approximation of the parton shower but the angular information is taken from the matrix element. This approach has been compared from a variety of implementations in [36]. Care has to be taken when the resolution scale of a jet algorithm to determine the number of hard jets above the merging scale and the merging scale itself don't concide in their physical meaning. In addition, it is possible that the parton shower applied to fill in the radiation below the merging scale is evolved in a scale with a different physical meaning than the merging scale. The resulting problems are usually seen as bumps inside distributions which are not washed out on the parton level [37]. To gain overall consistency one has to apply so-called truncated showers in order to fill the parton shower phase space properly, particularly for soft, wide-angle emissions [38, 39]. Apart from the overall normalization of all distributions which is formally still leading order, the accuracy of spectra for multiple jets is very remarkable. Shapes of high multiplicity events are reproduced in great detail where parton shower only descriptions are clearly seen to fail.

Fig. 6 shows histograms of the scale at which an event switches from a two-jet to a three-jet event in the Durham k_T-jet algorithm. The dashed vertical line denotes the matching scale $Q_{\rm ini}$. In the upper panel one can clearly see an imbalance of the contributions above and below the matching scale, which is due to the lack of truncated showers. In the lower panel, the truncated shower is applied and it is ensured that all available phase space is populated properly, hence the two contributions are matched much more smoothly. The same observable is shown in Fig. 7 against LEP data with an uncertainty band that results from variations of the argument of α_S and $Q_{\rm ini}$. The agreement and stability are quite remarkable.

The same algorithm, applied to hadronic collisions gives matching of similar quality. Fig. 8 shows the multiplicity of additional jets in W plus jet events at the Tevatron against data. One should note that the histogram is normalized such that the first bin is correct, as the Monte Carlo (at LO) is not intended to describe the overall normalization. The higher multiplicities are matched very well and it is clearly seen that the parton shower alone fails to describe this data.

4. Next-to-leading order

In a case quite complementary to the multi-jet case above, where only one extra emission is of interest but the overall normalization is supposed to be more accurate it is important to match the MC simulation to a next-to-leading order (NLO) matrix element. The arising problem is that extra hard radiation can be generated from the real correction matrix element as well as from the parton shower which leads us to a double counting problem.

Let us consider the way out in more detail. An Observable O may be described at NLO quite symbolically

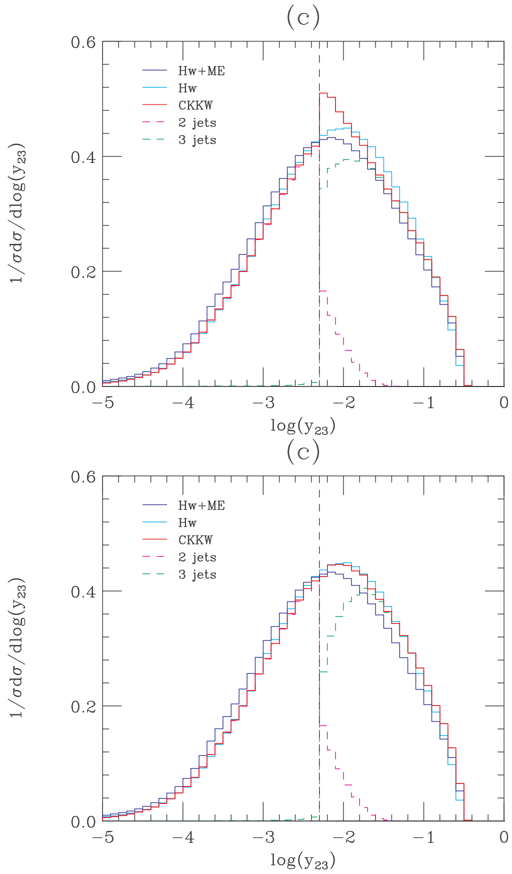

Figure 6: y_{23} distributions at LEP on the parton level, without (upper) and with truncated showers [39].

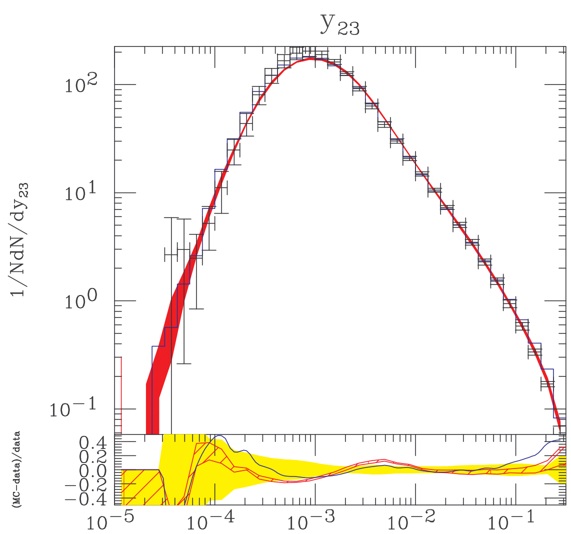

Figure 7: y_{23} distribution at LEP compared to the simulation with truncated showers. The red band results from variations in scales [39].

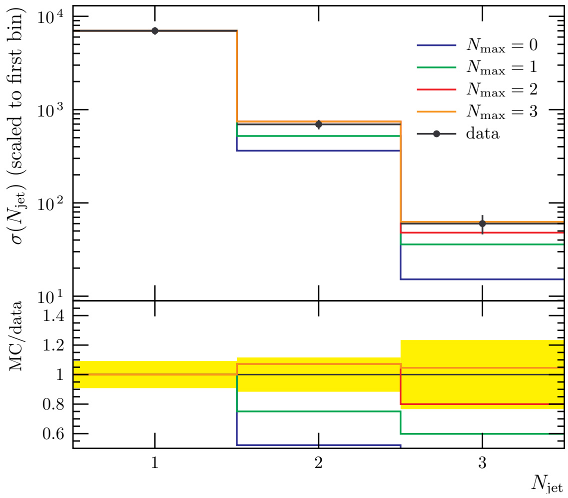

Figure 8: Multiplicity of additional jets in W events compared to SHERPA [38].

via the following contributions,

$$\langle O \rangle = O(0)\left[B + \bar{V}\right] + \int dx O(x) \frac{R(x) - A(x)}{x} . \quad (1)$$

Here, B denotes the Born level contribution. $R(x)$ is the squared real correction matrix element, depending on some real emission phase space variable x, with the divergent behaviour $1/x$ factored out. The limit $x \to 0$ denotes the usual infrared divergent limit, where the emitted particle becomes collinear or soft. $A(x)$ is an arbitrary subtraction term which is sufficiently regular and has the property $A(0) = R(0)$ such that the logarithmically divergent contribution from the integral becomes finite. Furthermore, $A(x)$ is chosen sufficiently simple in order to be integrated over the phase space x analytically, exhibiting the singular structure e.g. in terms of a dimensional regularization parameter. Then, $\bar{V}$ is the virtual correction plus the integrated subtraction term, such that all infrared divergences have been canceled. Thus far, this procedure is known as subtraction method and used in many recent NLO calculations [20, 40].

When applying a Monte Carlo simulation with the hard process taken from either a Born kinematic configuration ($x = 0$) or a real emission configuration we add in an extra contribution that is proportional to the splitting function $P(x)$ that will also contribution to the full NLO result, when expanded together with the Born configuration. Therefore, one may modify the description of the observable as

$$\langle O\rangle_{\rm MCNLO} = O(0)\left[B + \bar{V} + \int dx \frac{P(x) - A(x)}{x}\right] + \int dx O(x)\frac{R(x) - P(x)}{x}\,. \quad (2)$$

Now, if the parton shower is applied to either the Born type configuration (first line) or the real emission contribution (second line), the respective contributions from the splitting functions cancel on average with those from the parton shower and we have formally arrived at a proper NLO description of the observable. The freedom we still have is, apart from the right soft and collinear limits, the choice of the exact form of $A(x)$ and of the splitting function, that is, however, given by the parton shower implementation to be matched. We can now discuss the solutions of the double counting problem that have come up in the literature along the lines of Eq. (2).

The pioneering paper on matching parton showers and NLO calculations was [41]. There, the idea was to take the parton shower at face value, i.e. $P(x)$ was worked out from the Fortran HERWIG (fHERWIG) parton shower and a convenient subtraction scheme (the FKS scheme [42]) was used. Looking at Eq. (2), no particular simplification was achieved, but the integral in the first line had to be calculated only once and for all for the given parton shower algorithm. This had soon been extended to heavy particles [43] and was also worked out for more complicated processes [44, 45, 46]. By now, the list of available processes is quite long [47] and all processes are also available for the latest HERWIG++ parton shower [48]. Fig. 9 shows a comparison of the b quark transverse momentum relative to the parent t quark in $t\bar{t}$ production, simulated in MC@NLO, once with fHERWIG and once with HERWIG++.

The second method which is now very frequently used to match parton showers and NLO calculations is called POWHEG (positive weight hard emission generator) method because is overcomes the necessity of a small number of negative events. It is apparent from the observation that Eq. (2) simplifies significantly whenever not a given parton shower is used but the first emission is constructed from a parton shower based entirely on the real emission matrix element, i.e. $P(x) = R(x)$. In this case, the second line in Eq. (2) vanishes and hence we only produce Born type events with weights given by the inclusive NLO cross section Eq. (1). From there, a single parton shower emission is constructed from a special Sudakov form factor that contains the full $R(x)$ rather than the much simpler splitting function. As this generation may be computationally quite intensive, it is only applied for the first hard emission. All subsequent emissions are formally beyond NLO and hence here the usual parton shower can be used. The method was first reported in [49] and soon extended to more complicated processes [50, 51, 52, 53, 54, 55]. All processes are available via a single program package [56]. The POWHEG method has also been used early on by the HERWIG collaboration to implement a large number of processes, first as external packages [57, 58] and now for processes of varying complexity with the regular released version of HERWIG [59, 60, 61, 62]. Fig. 10 shows the transverse energy flow in deep inelastic scattering versus H1 data. The matrix element correction is clearly needed, while the NLO matched result improves the stability of the prediction. The accurate information on the addition of hard emission from the NLO calculation becomes vital in the distribution of a 3rd central jet in Higgs production events via vector boson fusion. This can clearly be seen in Fig. 11.

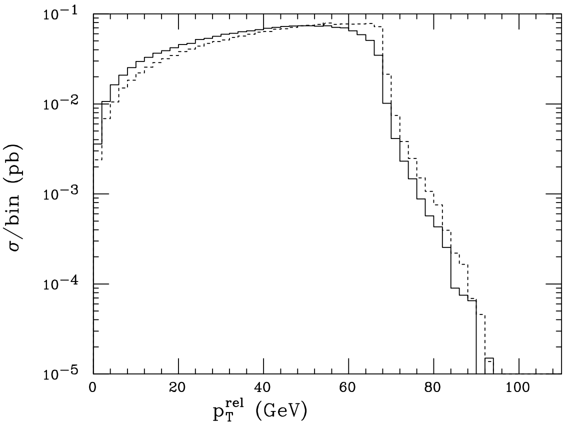

Figure 9: b quark transverse momentum relative to t quark in $t\bar{t}$ production [48]. HERWIG++ (solid) vs fHERWIG (dashed).

In addition to the above methods, from Eq. (2) we find another significant simplification if a custom parton shower is implemented such that $P(x) = A(x)$. In this case, the integral in the first line vanishes and the second line is exactly the subtracted real contribution that is normally calculated in every NLO program that uses the subtraction method. As already mentioned above, a number of parton showers have been implemented using the Catani–Seymour subtraction kernels [19, 23, 24]. Despite the fact that these showers have a number of advantages due to the accurate shower kinematics and the good approximation of matrix elements in the phase space away from the collinear limit, the original motivation to use the subtraction kernels as shower kernels is that the NLO matching becomes trivial for the above

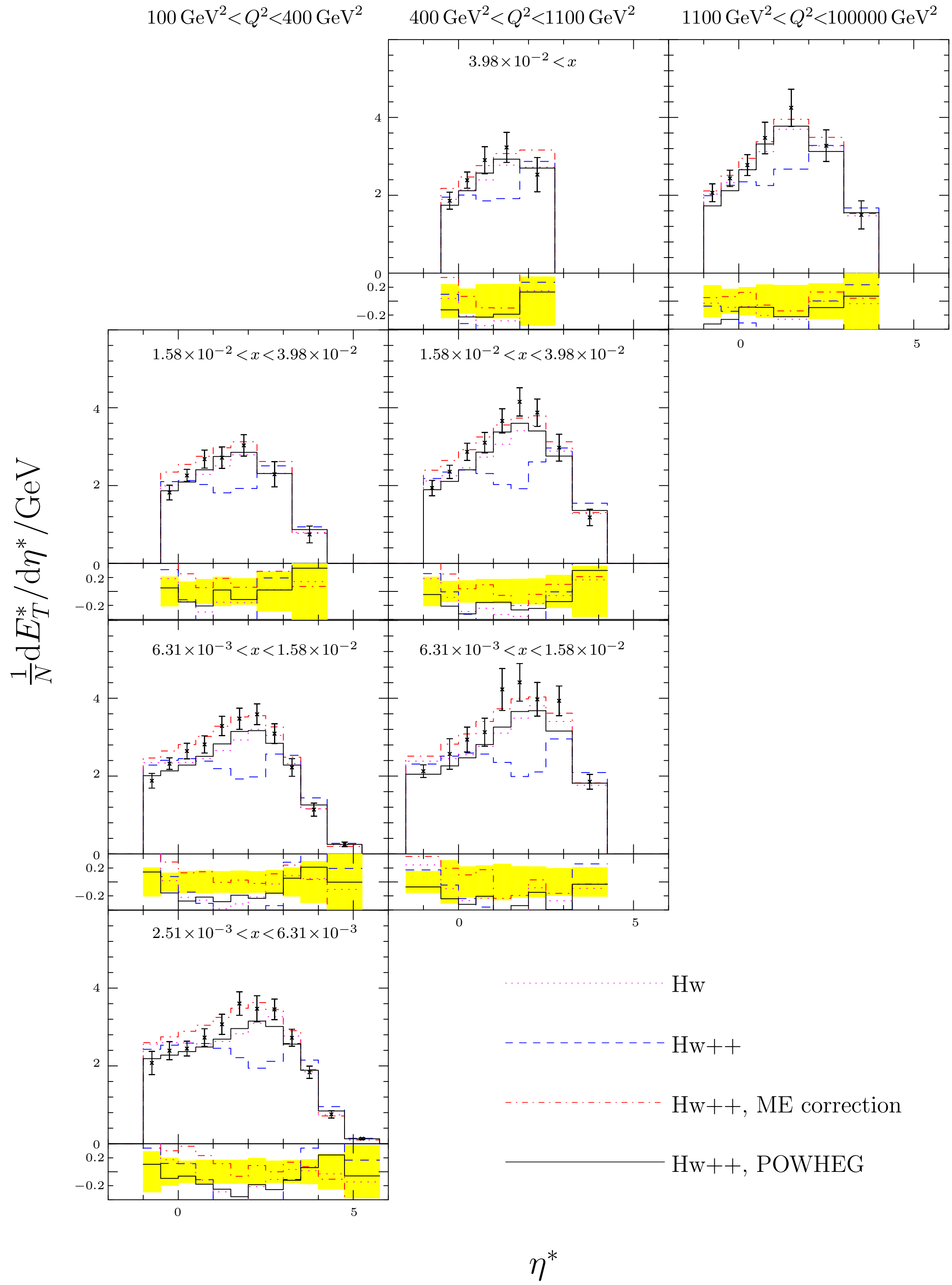

Figure 10: Energy flow versus pseudorapidity in DIS events [62].

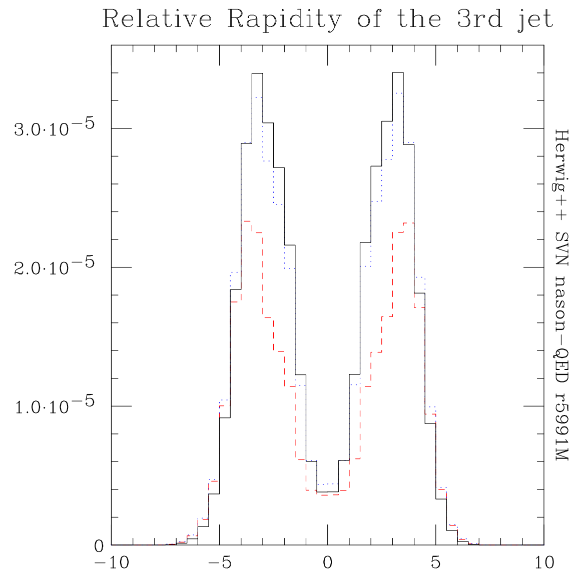

Figure 11: Rapidity of the 3rd jet relative to the two tagging jets in VBF Higgs production [62]. Shown are simulations at LO (dashes), with matrix element correction (dots) and NLO matched (solid).

reasons. Both, the POWHEG and the MC@NLO method have been used in SHERPA [63] and HERWIG [24] to match dipole showers to NLO calculations. In both cases, an automated matching to existing calculations is intended, e.g. by using the well-defined format for NLO output [64]. A critical comparison of the two methods can be found in [65]. It should be noted that particularly the POWHEG method may be problematic when used with a parton shower that is not ordered in the same transverse momentum that is used for the definition of 'hardness' in this approach. Fig. 12 depicts this situation for a p_T ordered shower (above) and an angular shower (below). In the first case, the hardest emission is generated first and all subsequent emissions have a smaller p_T, albeit not ordered in emission angle. In the latter case the hardest emission is entered into the middle of an angular ordered cascade. This situation can only be achieved if the softer, large angle emissions are inserted afterwards but *before* the hard emission. Otherwise, the colour structure will be disordered resulting e.g. in a different multiplicity of charged particles inside the jet that is generated by the parton in question. This truncated shower is always included in the internal implementations of the NLO matched processes. Additional instabilities might be expected when considering Fig. 13. Despite the fact that both approaches are formally accurate to NLO, the MC@NLO and POWHEG results differ quite significantly. Additionally the LO curve clearly indicates that some portion of phase space for the LO

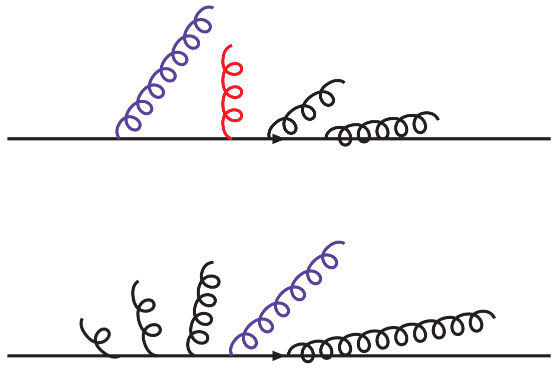

Figure 12: Sketch of parton showers and subsequent hard emission in p_T ordering (above) and angular ordering (below).

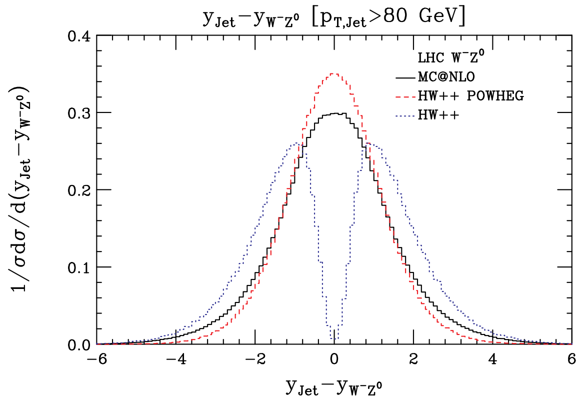

Figure 13: Rapidity of the additional jet relative to the vector boson pair in W^-Z^0 production [66].

parton shower is missed to be filled, hence the large gap at central rapidities. Research towards the differences of the two matching approaches is carried out in [65]. Fig. 14 illustrates that the new information gained from NLO matching as opposed to ME+PS merging can be the stability of the overall normalization. A simple K factor is introduced for ME+PS result. Once again, the parton shower alone doesn't populate all physically available phase space.

Recently, the two methods to merge matrix elements with different multiplicities with parton showers and to match NLO calculations with parton showers have been combined to give a result that benefits both from the increased accuracy of the overall normalization and reduced scale uncertainties from the NLO matching and the increased accuracy in the description of large angle or large transverse momentum emissions [67]. The proposed method (MENLOPS) has been tested with PYTHIA [68] and also has been implemented in the SHERPA package [69]. Figs. 15 and 16 show results obtained with this

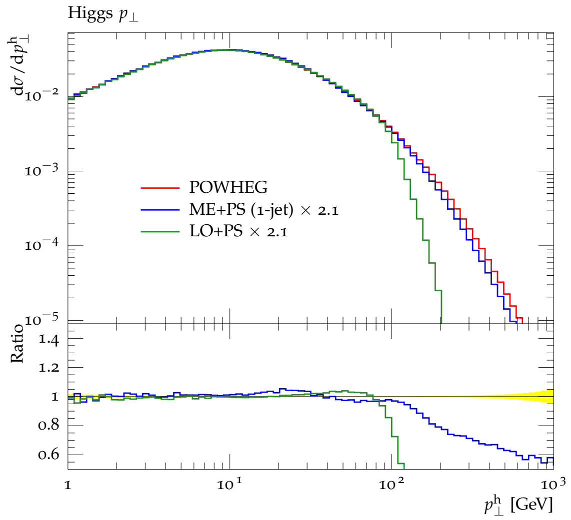

Figure 14: The transverse momentum of the Higgs boson in $gg \to h^0$, comparison of the POWHEG method with ME+PS merging and LO plus parton shower alone [63].

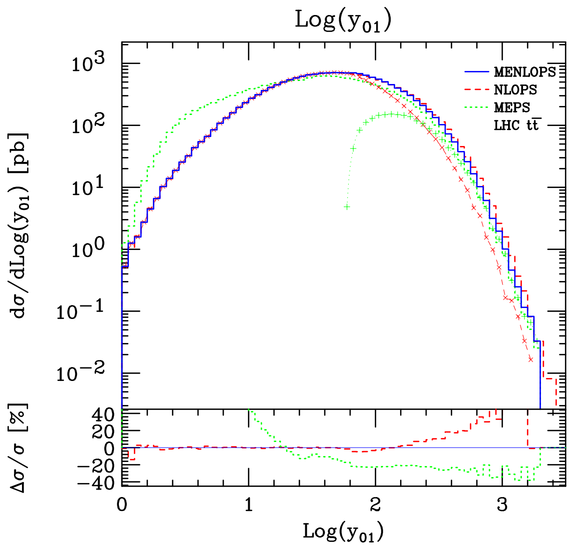

Figure 15: Distribution of the merging scale y_{01} from 0 to 1 jets in $t\bar{t}$ plus jet events [68].

advanced matching and merging. Fig. 16 shows that the MENLOPS approach gives a similar shape as the ME+PS matched simulation while offering a more reliable prediction of the normalization which is simply put in by hand for the LO result. The NLO alone gives a much softer tail of the H_T distribution.

5. Hadronization and decays

The hadronization models in the discussed event generators have not changed much in the physical details with respect to the implementations in the respective Fortran programs. SHERPA has implemented a newly developed cluster hadronization model that is in many aspects quite similar to the cluster hadronization in HERWIG but differs in details and has a few extensions [70].

The implementation of hadronic decays is very different from those in the Fortran programs. The photon radiation in the decay of hadrons is much more sophisticated and allows for multiple emissions, accurate to higher orders [71, 72]. In addition, the decays of τ mesons [73] and other hadrons is modeled in much greater detail than before, reaching or even surpassing the level of sophistication of dedicated decay packages.

6. Multiple partonic interactions

An important component in the modeling of high energy hadronic interactions is the underlying event (UE). It is now established that most of the activity that is not attributed directly to the hard process stems from additional (semi-) hard partonic scatters, so-called multiple partonic interactions (MPI). A first model, on which most of the implementations are footed was formulated in [74] and was the main model in PYTHIA for a long time. Models based on the assumptions made there, are implemented recently in HERWIG and SHERPA. In recent PYTHIA versions, however, the additional hard scatters are interleaved with the parton shower [17, 18] such that a different picture of an evolution in p_T space emerges. New developments in SHERPA aim at a smooth inclusion of diffractive and soft interactions into the multiple interaction picture, based on a Gribov–Regge–approach [75]. In Fortan HERWIG the UE had been modeled in an additional package JIMMY [76] that has added additional hard scatters to the HERWIG simulation. This model had also been studied with an additional soft component [77]. Models similar to this hard and soft component of multiple partonic interactions are now part of the HERWIG++ implementation [78, 79].

With the advent of first LHC data it was soon realized that the model needs an additional mechanism for colour reconnections. The hard multiple interactions are correlated arbitrarily in colour space which is unphysical. Due to colour preconfinement one expects the different scatters to be correlated such that neighboring partons in momentum space are also close to each other in colour space. As neighbours in momentum space may as well stem from a different hard interaction in the MPI model it must be possible that the colour con-

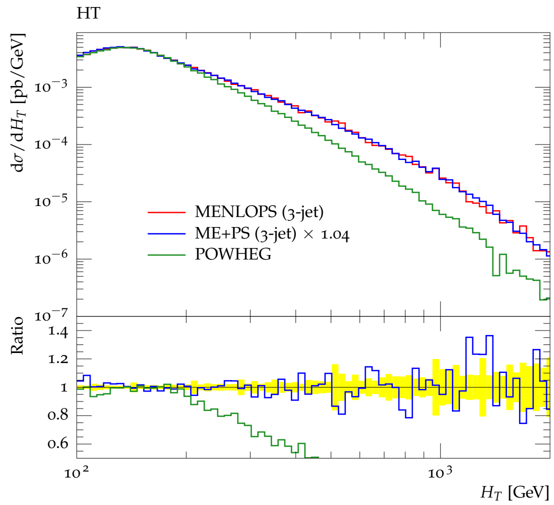

Figure 16: H_T distribution in *WW* events, comparison of MENLOPS, POWHEG and ME+PS merging [69].

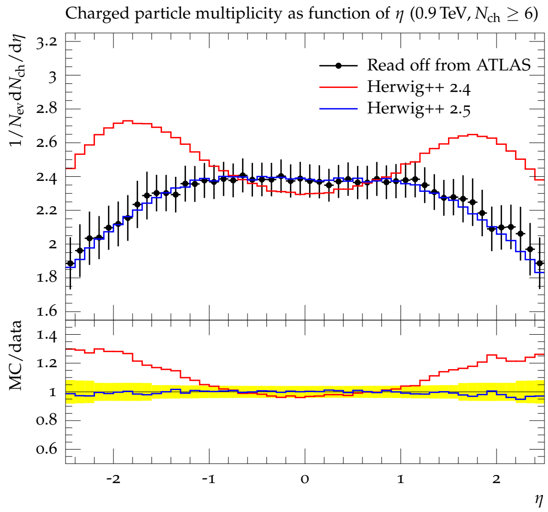

Figure 17: Charged particle rapidity distribution in minimum bias events with $N_{\mathrm{ch}} \geq 6$. HERWIG++ 2.5 includes the colour reconnection model, HERWIG++ 2.4 doesn't.

nections are reshuffled via the exchange of soft gluons such that an overall tension between all colour strings is somewhat minimized. This effect was already studied at LEP where it could be expected in *W* pair production events (see e.g. [80]) but was found to be insignificant. At hadron colliders the situation is quite different. Implications for the the top mass determination were studied in [81].

The implementation of a colour reconnection model in HERWIG minimizes the 'colour length' λ which is the sum of the invariant masses of all clusters after the parton shower $\lambda = \sum m^2_{\mathrm{cluster}}$. In order to minimize or reduce this sum, all clusters are iterated and for a second random cluster is is checked whether a swap in colour charges would reduce λ. If so, this is done with a certain probability. It is indeed found that this algorithm leads to much more physical results (Figs. 17 and 18).

With this model, tunes of minimum bias and underlying event data from the LHC (900 GeV and 7 TeV) and the Tevatron have been performed. The underlying event is usually measured in dijet events. Here, the azimuthal region transverse to the two jets is selected and the density of charged particles and the transverse momentum flow are measured. It is found that in the transverse region the activity is quite uncorrelated to the leading jets themselves. Fig. 19 shows the density of charged particles with respect to $\Delta\phi$, the angle between the leading jet and the additional particles. The activity in the transverse region is clearly depleted ($\pi/3 < \phi < 2\pi/3$). Fig. 20 shows nicely that the transverse activity decouples from the leading jet momentum for large momenta, as a plateau is formed, hence the correct interpretation as underlying event activity. Fig. 21 shows the correlation between transverse momentum and N_{ch} which is very sensitive to the colour structure of the event.

7. Conclusion

A lot of progress has been made in the development of Monte Carlo event generators. The 'new' event generators HERWIG++, PYTHIA and SHERPA are by now probably superior to the Fortran predecessors and offer a variety of new features. Recently, most progress is being made in the area of improving the perturbative description of events, nevertheless, there are still important non-perturbative physics questions like the modelling of multiple partonic interactions that are very relevant for an accurate description of collider data.

Acknowledgements

I would like to thank the organizers for the kind invitation to this very pleasant and fruitful workshop. This work was supported in part by the Helmholtz Alliance "Physics at the Terascale".

References

[1] G. Corcella, I. Knowles, G. Marchesini, S. Moretti, K. Odagiri, et al., HERWIG 6: An Event generator for hadron emission reactions with interfering gluons (including supersymmetric processes), JHEP 0101 (2001) 010. arXiv:hep-ph/0011363.

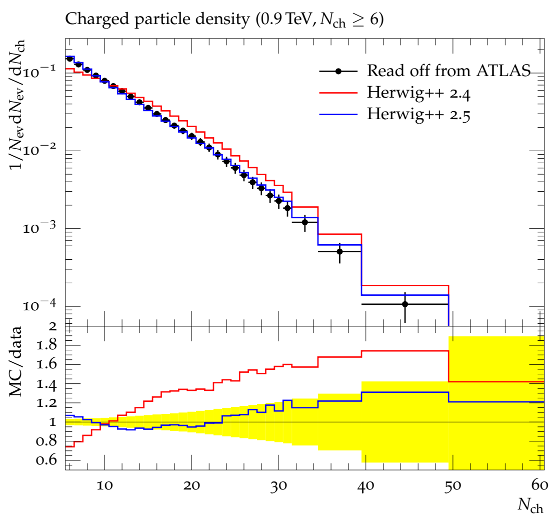

Figure 18: Multiplicity of Charged particles in minimum bias events with $N_{ch} \geq 6$. HERWIG++ 2.5 includes the colour reconnection model, HERWIG++ 2.4 doesn't.

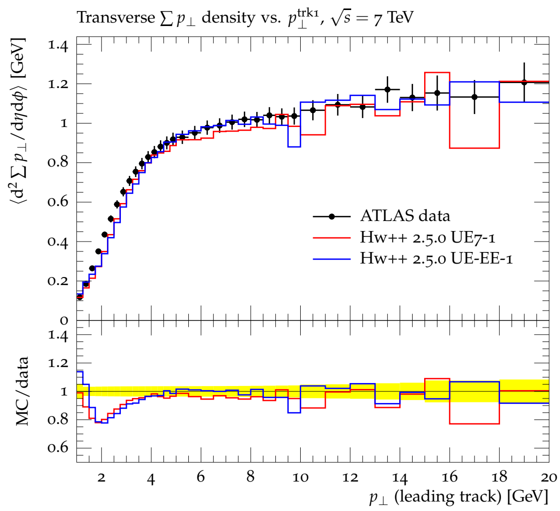

Figure 20: Transverse Σp_T density in dijet events at 7 TeV.

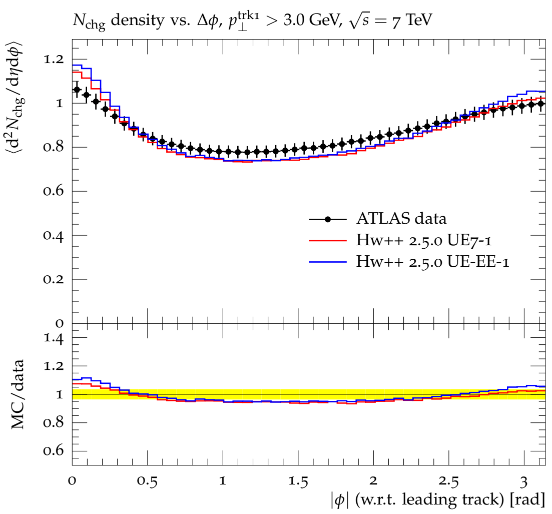

Figure 19: N_{chg} density vs $\Delta\phi$ in dijet events at 7 TeV.

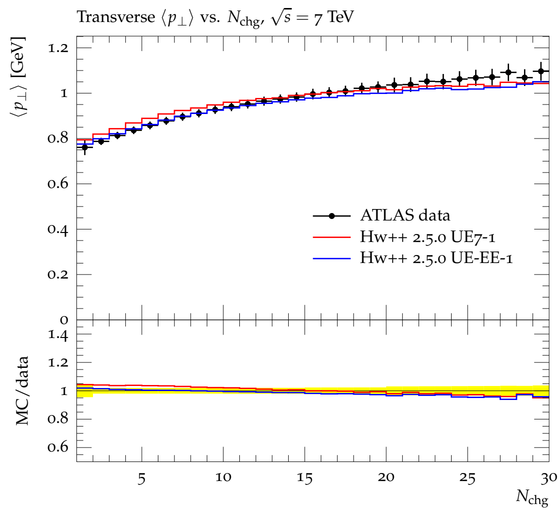

Figure 21: $\langle p_T \rangle$ vs N_{chg} in dijet events at 7 TeV.

[2] G. Corcella, et al., HERWIG 6.5 release note arXiv:hep-ph/0210213.

[3] T. Sjöstrand, S. Mrenna, P. Skands, PYTHIA 6.4 Physics and Manual, JHEP 05 (2006) 026. arXiv:hep-ph/0603175.

[4] M. Bähr et al., Herwig++ Physics and Manual, Eur. Phys. J. C58 (2008) 639–707. arXiv:0803.0883, doi:10.1140/epjc/s10052-008-0798-9.

[5] T. Sjöstrand, S. Mrenna, P. Skands, A Brief Introduction to PYTHIA 8.1, Comput. Phys. Commun. 178 (2008) 852–867. arXiv:0710.3820, doi:10.1016/j.cpc.2008.01.036.

[6] T. Gleisberg, et al., SHERPA 1.alpha, a proof-of-concept version, JHEP 02 (2004) 056. arXiv:hep-ph/0311263.

[7] T. Gleisberg, et al., Event generation with SHERPA 1.1, JHEP 02 (2009) 007. arXiv:0811.4622, doi:10.1088/1126-6708/2009/02/007.

[8] T. Gleisberg, S. Hoeche, Comix, a new matrix element generator, JHEP 0812 (2008) 039. arXiv:0808.3674, doi:10.1088/1126-6708/2008/12/039.

[9] F. Krauss, R. Kuhn, G. Soff, AMEGIC++ 1.0: A Matrix element generator in C++, JHEP 0202 (2002) 044. arXiv:hep-ph/0109036.

[10] M. Gigg, P. Richardson, Simulation of beyond standard model physics in Herwig++, Eur. Phys. J. C51 (2007) 989–1008. arXiv:hep-ph/0703199, doi:10.1140/epjc/s10052-007-0364-x.

[11] M. Gigg, P. Richardson, Simulation of Finite Width Effects in Physics Beyond the Standard Model arXiv:0805.3037.

[12] N. Desai, P.Z. Skands, Supersymmetry and Generic BSM Models in PYTHIA 8 arXiv:1109.5852.

[13] P. Richardson, Spin correlations in Monte Carlo simulations, JHEP 0111 (2001) 029. arXiv:hep-ph/0110108.

[14] J. Alwall, M. Herquet, F. Maltoni, O. Mattelaer, T. Stelzer, MadGraph 5 : Going Beyond, JHEP 1106 (2011) 128. arXiv:1106.0522, doi:10.1007/JHEP06(2011)128.

[15] J. Alwall, A. Ballestrero, P. Bartalini, S. Belov, E. Boos, et al., A Standard format for Les Houches event files, Comput. Phys. Commun. 176 (2007) 300–304. arXiv:hep-ph/0609017, doi:10.1016/j.cpc.2006.11.010.

[16] S. Gieseke, P. Stephens and B.R. Webber, New formalism for QCD parton showers, JHEP 12 (2003) 045. arXiv:hep-ph/0310083.

[17] T. Sjöstrand, P.Z. Skands, Multiple interactions and the structure of beam remnants, JHEP 03 (2004) 053. arXiv:hep-ph/0402078.

[18] T. Sjöstrand, P.Z. Skands, Transverse-momentum-ordered showers and interleaved multiple interactions, Eur. Phys. J. C39 (2005) 129–154. arXiv:hep-ph/0408302, doi:10.1140/epjc/s2004-02084-y.

[19] S. Schumann, F. Krauss, A Parton shower algorithm based on Catani-Seymour dipole factorisation, JHEP 03 (2008) 038. arXiv:0709.1027, doi:10.1088/1126-6708/2008/03/038.

[20] S. Catani and M.H. Seymour, A general algorithm for calculating jet cross sections in NLO QCD, Nucl. Phys. B485 (1997) 291–419. arXiv:hep-ph/9605323, doi:10.1016/S0550-3213(96)00589-5.

[21] J.C. Winter, F. Krauss, Initial-state showering based on colour dipoles connected to incoming parton lines, JHEP 07 (2008) 040. arXiv:0712.3913, doi:10.1088/1126-6708/2008/07/040.

[22] L. Lönnblad, ARIADNE version 4: A Program for simulation of QCD cascades implementing the color dipole model, Comput. Phys. Commun. 71 (1992) 15–31. doi:10.1016/0010-4655(92)90068-A.

[23] M. Dinsdale, M. Ternick and S. Weinzierl, Parton showers from the dipole formalism, Phys. Rev. D76 (2007) 094003. arXiv:0709.1026, doi:10.1103/PhysRevD.76.094003.

[24] S. Platzer, S. Gieseke, Dipole Showers and Automated NLO Matching in Herwig++ arXiv:1109.6256.

[25] W.T. Giele, D.A. Kosower, P.Z. Skands, A Simple shower and matching algorithm, Phys. Rev. D78 (2008) 014026. arXiv:0707.3652, doi:10.1103/PhysRevD.78.014026.

[26] W. Giele, D. Kosower, P. Skands, Higher-Order Corrections to Timelike Jets, Phys.Rev. D84 (2011) 054003. arXiv:1102.2126, doi:10.1103/PhysRevD.84.054003.

[27] A. Gehrmann-De Ridder, M. Ritzmann, P. Skands, Timelike Dipole-Antenna Showers with Massive Fermions arXiv:1108.6172.

[28] V. Khachatryan, et al., First Measurement of Hadronic Event Shapes in pp Collisions at sqrt(s)=7 TeV, Phys. Lett. B699 (2011) 48–67. arXiv:1102.0068, doi:10.1016/j.physletb.2011.03.060.

[29] [link].
URL `http://mcplots.cern.ch`

[30] G. Aad, et al., Study of Jet Shapes in Inclusive Jet Production in pp Collisions at sqrt(s) = 7 TeV using the ATLAS Detector, Phys. Rev. D83 (2011) 052003, long author list - awaiting processing. arXiv:1101.0070, doi:10.1103/PhysRevD.83.052003.

[31] M.H. Seymour, Matrix element corrections to parton shower algorithms, Comput. Phys. Commun. 90 (1995) 95–101. arXiv:hep-ph/9410414, doi:10.1016/0010-4655(95)00064-M.

[32] E. Norrbin, T. Sjöstrand, QCD radiation off heavy particles, Nucl. Phys. B603 (2001) 297–342. arXiv:hep-ph/0010012, doi:10.1016/S0550-3213(01)00099-2.

[33] S. Catani, F. Krauss, R. Kuhn, B.R. Webber, QCD Matrix Elements + Parton Showers, JHEP 11 (2001) 063. arXiv:hep-ph/0109231.

[34] F. Krauss, Matrix elements and parton showers in hadronic interactions, JHEP 08 (2002) 015. arXiv:hep-ph/0205283.

[35] L. Lönnblad, Correcting the colour-dipole cascade model with fixed order matrix elements, JHEP 05 (2002) 046. arXiv:hep-ph/0112284.

[36] J. Alwall, et al., Comparative study of various algorithms for the merging of parton showers and matrix elements in hadronic collisions, Eur. Phys. J. C53 (2008) 473–500. arXiv:0706.2569, doi:10.1140/epjc/s10052-007-0490-5.

[37] N. Lavesson, L. Lönnblad, Merging parton showers and matrix elements – back to basics, JHEP 04 (2008) 085. arXiv:0712.2966, doi:10.1088/1126-6708/2008/04/085.

[38] S. Hoeche, F. Krauss, S. Schumann, F. Siegert, QCD matrix elements and truncated showers, JHEP 05 (2009) 053. arXiv:0903.1219, doi:10.1088/1126-6708/2009/05/053.

[39] K. Hamilton, P. Richardson, J. Tully, A Modified CKKW matrix element merging approach to angular-ordered parton showers, JHEP 0911 (2009) 038. arXiv:0905.3072, doi:10.1088/1126-6708/2009/11/038.

[40] S. Catani, S. Dittmaier, M.H. Seymour, Z. Trocsanyi, The dipole formalism for next-to-leading order QCD calculations with massive partons, Nucl. Phys. B627 (2002) 189–265. arXiv:hep-ph/0201036, doi:10.1016/S0550-3213(02)00098-6.

[41] S. Frixione, B.R. Webber, Matching NLO QCD computations and parton shower simulations, JHEP 06 (2002) 029. arXiv:hep-ph/0204244.

[42] S. Frixione, Z. Kunszt, A. Signer, Three jet cross-sections to next-to-leading order, Nucl. Phys. B467 (1996) 399–442. arXiv:hep-ph/9512328, doi:10.1016/0550-3213(96)00110-1.

[43] S. Frixione, P. Nason, B.R. Webber, Matching NLO QCD and parton showers in heavy flavour production, JHEP 08 (2003) 007. arXiv:hep-ph/0305252.

[44] S. Frixione, E. Laenen, P. Motylinski, B.R. Webber, Single-top production in MC@NLO, JHEP 03 (2006) 092. arXiv:hep-ph/0512250.

[45] S. Frixione, E. Laenen, P. Motylinski, B.R. Webber, Angular correlations of lepton pairs from vector boson and top

quark decays in Monte Carlo simulations, JHEP 04 (2007) 081. arXiv:hep-ph/0702198.

[46] S. Frixione, E. Laenen, P. Motylinski, B.R. Webber, C.D. White, Single-top hadroproduction in association with a W boson, JHEP 07 (2008) 029. arXiv:0805.3067, doi:10.1088/1126-6708/2008/07/029.

[47] S. Frixione, F. Stoeckli, P. Torrielli, B.R. Webber, C.D. White, The MC@NLO 4.0 Event Generator arXiv:1010.0819.

[48] S. Frixione, F. Stoeckli, P. Torrielli, B.R. Webber, NLO QCD corrections in Herwig++ with MC@NLO, JHEP 1101 (2011) 053. arXiv:1010.0568, doi:10.1007/JHEP01(2011)053.

[49] P. Nason, A new method for combining NLO QCD with shower Monte Carlo algorithms, JHEP 11 (2004) 040. arXiv:hep-ph/0409146, doi:10.1088/1126-6708/2004/11/040.

[50] P. Nason, G. Ridolfi, A positive-weight next-to-leading-order Monte Carlo for Z pair hadroproduction, JHEP 08 (2006) 077. arXiv:hep-ph/0606275.

[51] S. Frixione, P. Nason, G. Ridolfi, A Positive-Weight Next-to-Leading-Order Monte Carlo for Heavy Flavour Hadroproduction, JHEP 09 (2007) 126. arXiv:0707.3088, doi:10.1088/1126-6708/2007/09/126.

[52] S. Frixione, P. Nason, C. Oleari, Matching NLO QCD computations with Parton Shower simulations: the POWHEG method, JHEP 11 (2007) 070. arXiv:0709.2092, doi:10.1088/1126-6708/2007/11/070.

[53] S. Alioli, P. Nason, C. Oleari, E. Re, NLO vector-boson production matched with shower in POWHEG, JHEP 07 (2008) 060. arXiv:0805.4802, doi:10.1088/1126-6708/2008/07/060.

[54] S. Alioli, P. Nason, C. Oleari, E. Re, NLO Higgs boson production via gluon fusion matched with shower in POWHEG, JHEP 04 (2009) 002. arXiv:0812.0578, doi:10.1088/1126-6708/2009/04/002.

[55] S. Alioli, K. Hamilton, P. Nason, C. Oleari, E. Re, Jet pair production in POWHEG, JHEP 1104 (2011) 081. arXiv:1012.3380, doi:10.1007/JHEP04(2011)081.

[56] S. Alioli, P. Nason, C. Oleari, E. Re, A general framework for implementing NLO calculations in shower Monte Carlo programs: the POWHEG BOX, JHEP 1006 (2010) 043. arXiv:1002.2581, doi:10.1007/JHEP06(2010)043.

[57] O. Latunde-Dada, S. Gieseke, B.R. Webber, A positive-weight next-to-leading-order Monte Carlo for e+ e- annihilation to hadrons, JHEP 02 (2007) 051. arXiv:hep-ph/0612281.

[58] O. Latunde-Dada, Applying the POWHEG method to top pair production and decays at the ILC, Eur. Phys. J. C58 (2008) 543–554. arXiv:0806.4560, doi:10.1140/epjc/s10052-008-0785-1.

[59] K. Hamilton, P. Richardson, J. Tully, A Positive-Weight Next-to-Leading Order Monte Carlo Simulation of Drell-Yan Vector Boson Production, JHEP 10 (2008) 015. arXiv:0806.0290, doi:10.1088/1126-6708/2008/10/015.

[60] K. Hamilton, P. Richardson, J. Tully, A Positive-Weight Next-to-Leading Order Monte Carlo Simulation for Higgs Boson Production, JHEP 04 (2009) 116. arXiv:0903.4345, doi:10.1088/1126-6708/2009/04/116.

[61] L. D'Errico, P. Richardson, Next-to-Leading-Order Monte Carlo Simulation of Diphoton Production in Hadronic Collisions, arXiv:1106.3939.

[62] L. D'Errico, P. Richardson, A Positive-Weight Next-to-Leading-Order Monte Carlo Simulation of Deep Inelastic Scattering and Higgs Boson Production via Vector Boson Fusion in Herwig++, arXiv:1106.2983.

[63] S. Hoche, F. Krauss, M. Schonherr, F. Siegert, Automating the POWHEG method in Sherpa, JHEP 1104 (2011) 024. arXiv:1008.5399, doi:10.1007/JHEP04(2011)024.

[64] T. Binoth, F. Boudjema, G. Dissertori, A. Lazopoulos, A. Denner, et al., A Proposal for a standard interface between Monte Carlo tools and one-loop programs, Comput. Phys. Commun. 181 (2010) 1612–1622, dedicated to the memory of, and in tribute to, Thomas Binoth, who led the effort to develop this proposal for Les Houches 2009. arXiv:1001.1307, doi:10.1016/j.cpc.2010.05.016.

[65] S. Hoeche, F. Krauss, M. Schonherr, F. Siegert, A critical appraisal of NLO+PS matching methods, arXiv:1111.1220.

[66] K. Hamilton, A positive-weight next-to-leading order simulation of weak boson pair production, JHEP 1101 (2011) 009. arXiv:1009.5391, doi:10.1007/JHEP01(2011)009.

[67] N. Lavesson, L. Lönnblad, Extending CKKW-merging to One-Loop Matrix Elements, JHEP 12 (2008) 070. arXiv:0811.2912, doi:10.1088/1126-6708/2008/12/070.

[68] K. Hamilton, P. Nason, Improving NLO-parton shower matched simulations with higher order matrix elements, JHEP 1006 (2010) 039. arXiv:1004.1764, doi:10.1007/JHEP06(2010)039.

[69] S. Hoche, F. Krauss, M. Schonherr, F. Siegert, NLO matrix elements and truncated showers, JHEP 1108 (2011) 123. arXiv:1009.1127, doi:10.1007/JHEP08(2011)123.

[70] J.C. Winter, F. Krauss, G. Soff, A Modified cluster hadronization model, Eur. Phys. J. C36 (2004) 381–395. arXiv:hep-ph/0311085, doi:10.1140/epjc/s2004-01960-8.

[71] K. Hamilton, P. Richardson, Simulation of QED radiation in particle decays using the YFS formalism, JHEP 0607 (2006) 010. arXiv:hep-ph/0603034, doi:10.1088/1126-6708/2006/07/010.

[72] M. Schonherr, F. Krauss, Soft Photon Radiation in Particle Decays in SHERPA, JHEP 0812 (2008) 018. arXiv:0810.5071, doi:10.1088/1126-6708/2008/12/018.

[73] D. Grellscheid, P. Richardson, Simulation of Tau Decays in the Herwig++ Event Generator, arXiv:0710.1951.

[74] T. Sjöstrand, M. van Zijl, A Multiple Interaction Model for the Event Structure in Hadron Collisions, Phys. Rev. D36 (1987) 2019. doi:10.1103/PhysRevD.36.2019.

[75] V. Khoze, F. Krauss, A. Martin, M. Ryskin, K. Zapp, Diffraction and correlations at the LHC: Definitions and observables, Eur. Phys. J. C69 (2010) 85–93. arXiv:1005.4839, doi:10.1140/epjc/s10052-010-1392-5.

[76] J. Butterworth, J.R. Forshaw, M.H. Seymour, Multiparton interactions in photoproduction at HERA, Z. Phys. C72 (1996) 637–646. arXiv:hep-ph/9601371, doi:10.1007/s002880050286.

[77] I. Borozan, M. Seymour, An Eikonal model for multiparticle production in hadron hadron interactions, JHEP 0209 (2002) 015. arXiv:hep-ph/0207283.

[78] M. Bähr, S. Gieseke, M.H. Seymour, Simulation of multiple partonic interactions in Herwig++, JHEP 07 (2008) 076. arXiv:0803.3633, doi:10.1088/1126-6708/2008/07/076.

[79] M. Bähr, J.M. Butterworth, S. Gieseke, M.H. Seymour, Soft interactions in Herwig++, arXiv:0905.4671.

[80] J. Abdallah, et al., Investigation of colour reconnection in WW events with the DELPHI detector at LEP-2, Eur. Phys. J. C51 (2007) 249–269. arXiv:0704.0597, doi:10.1140/epjc/s10052-007-0304-9.

[81] P.Z. Skands, D. Wicke, Non-perturbative QCD effects and the top mass at the Tevatron, Eur. Phys. J. C52 (2007) 133–140. arXiv:hep-ph/0703081, doi:10.1140/epjc/s10052-007-0352-1.